



# Technical note: Introduction of a superconducting gravimeter as novel hydrological sensor for the Alpine research catchment Zugspitze

Christian Voigt<sup>1</sup>, Karsten Schulz<sup>2</sup>, Franziska Koch<sup>2</sup>, Karl-Friedrich Wetzel<sup>3</sup>, Ludger Timmen<sup>4</sup>, Till Rehm<sup>5</sup>, Hartmut Pflug<sup>1</sup>, Nico Stolarczuk<sup>1</sup>, Christoph Förste<sup>1</sup>, and Frank Flechtner<sup>1,6</sup>

<sup>1</sup>Section 1.2 Global Geomonitoring and Gravity Field, GFZ German Research Centre for Geosciences, Telegrafenberg, 14473 Potsdam, Germany

<sup>2</sup>Institute for Hydrology and Water Management, University of Natural Resources and Life Sciences (BOKU), Muthgasse 18, 1190 Vienna, Austria

<sup>3</sup>Institute of Geography, Augsburg University, Alter Postweg 118, 86159 Augsburg, Germany

<sup>4</sup>Institute of Geodesy, Leibniz University Hannover (LUH), Schneiderberg 50, 30167 Hannover, Germany

<sup>5</sup>Environmental Research Station Schneefernerhaus (UFS), Zugspitze 5, 82475 Zugspitze, Germany

<sup>6</sup>Institute of Geodesy and Geoinformation Science, Technische Universität Berlin (TUB), Kaiserin-Augusta-Allee 104–106, 10553 Berlin, Germany

**Correspondence:** Christian Voigt (christian.voigt@gfz-potsdam.de)

Received: 5 February 2021 – Discussion started: 8 March 2021

Revised: 16 August 2021 – Accepted: 18 August 2021 – Published: 20 September 2021

**Abstract.** GFZ (German Research Centre for Geosciences) set up the Zugspitze Geodynamic Observatory Germany with a worldwide unique installation of a superconducting gravimeter at the summit of Mount Zugspitze on top of the Partnach spring catchment. This high alpine catchment is well instrumented, acts as natural lysimeter and has significant importance for water supply to its forelands, with a large mean annual precipitation of 2080 mm and a long seasonal snow cover period of 9 months, while showing a high sensitivity to climate change. However, regarding the majority of alpine regions worldwide, there is only limited knowledge on temporal water storage variations due to sparsely distributed hydrological and meteorological sensors and the large variability and complexity of signals in alpine terrain. This underlines the importance of well-equipped areas such as Mount Zugspitze serving as natural test laboratories for improved monitoring, understanding and prediction of alpine hydrological processes. The observatory superconducting gravimeter, OSG 052, supplements the existing sensor network as a novel hydrological sensor system for the direct observation of the integral gravity effect of total water storage variations in the alpine research catchment at

Zugspitze. Besides the experimental set-up and the available data sets, the gravimetric methods and gravity residuals are presented based on the first 27 months of observations from 29 December 2018 to 31 March 2021. The snowpack is identified as being a primary contributor to seasonal water storage variations and, thus, to the gravity residuals with a signal range of up to  $750 \text{ nm s}^{-2}$  corresponding to 1957 mm snow water equivalent measured with a snow scale at an altitude of 2420 m at the end of May 2019. Hydro-gravimetric sensitivity analysis reveal a snow–gravimetric footprint of up to 4 km distance around the gravimeter, with a dominant gravity contribution from the snowpack in the Partnach spring catchment. This shows that the hydro-gravimetric approach delivers representative integral insights into the water balance of this high alpine site.

## 1 Introduction

One of the grand societal challenges is ensuring sufficient water supply under climate change conditions. The European Alps are of crucial importance to supply water for ecologi-

cal, energy and societal purposes and, with a relatively large fraction of annual precipitation received and stored, they are often referred to as water towers (Immerzeel et al., 2020; Beniston et al., 2018; Viviroli et al., 2007). The IPCC (Intergovernmental Panel on Climate Change; 2014) indicates that “in many regions, changing precipitation or melting snow and ice are altering hydrological systems, affecting water resources in terms of quantity and quality”, thereby emphasising the need for efficient future water management strategies, even in currently water secure regions (Immerzeel et al., 2020). To develop such strategies, a comprehensive understanding and quantification of changing hydrological processes in mountainous regions, including short- and long-term observations and model predictions are urgently required.

However, due to the high installation and maintenance costs of monitoring equipment, and the often harsh environmental conditions causing instrument failure and difficult accessibility, hydro-meteorological observatories and subsequent data for high alpine catchments are scarce. The Partnach spring catchment (Fig. 1) in the southeast of the summit of Mount Zugspitze, also known as Research Catchment Zugspitze (RCZ), covers an area of about 11 km<sup>2</sup> located in the Northern Limestone Alps and is one of the best-instrumented high alpine catchments for monitoring snow hydrological processes (Bernhardt et al., 2018). Its main characteristics are a mean annual precipitation of 2080 mm, with 80 % as snowfall from autumn to late spring above approx. 1800 m and an average temperature of  $-4.5^{\circ}\text{C}$  during the climatic reference period 1981 to 2010 (Weber et al., 2016). The altitudes vary between 2962 m (summit of Mount Zugspitze) and 1430 m at Partnach spring.

The Partnach spring drains the entire RCZ due to a synclinal geological structure, with impermeable claystones underlying the highly karstified Wetterstein limestone, and can therefore be regarded as a natural lysimeter, allowing for detailed water balance and water movement studies (Wetzel, 2004; Rappl et al., 2010). Given this unique geological situation and the available instrumentation, the RCZ is part of the Global Energy and Water Exchanges (GEWEX) International Network of Alpine Research Catchments (INARCH; Pomeroy et al., 2015). The remains of Germany's highest glacier – the northern and southern Schneeferner – are also located in the RCZ (Hagg et al., 2012), as well as permafrost in the rock walls of Mount Zugspitze (Krautblatter et al., 2010). The RCZ is part of the Bockhütte catchment with an area of 25 km<sup>2</sup>. The Hammersbach catchment covers an area of 14 km<sup>2</sup> in a northeasterly direction from Mount Zugspitze and includes the Höllentalferner glacier. Karst hydrological characteristics can be found in Lauber and Goldscheider (2014).

The environmental research station Schneefernerhaus (UFS), located in the RCZ, is easily accessible with cable cars and operates a dense hydro-meteorological sensor network jointly with the German Weather Service (DWD) and

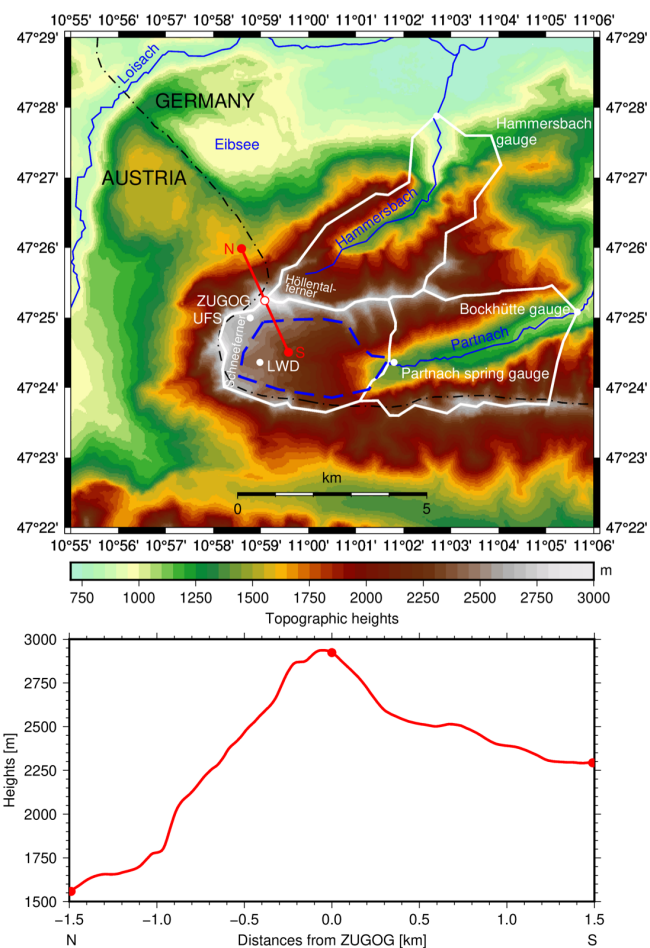


**Figure 1.** Topographic heights around the Zugspitze Geodynamic Observatory Germany (ZUGOG), the Environmental Research Station (UFS) and the hydro-meteorological station (LWD), the alpine catchments (white lines) and Partnach spring (11 km<sup>2</sup>) as part of Bockhütte (25 km<sup>2</sup>), with their corresponding gauge stations, and the Hammersbach catchment (14 km<sup>2</sup>), with its planned gauge station, the estimated groundwater body below Zugspitzplatt (blue dashed line) and a topographic north–south profile through ZUGOG transverse to the maximum slopes (red line).

the Bavarian Avalanche Warning Service (LWD), including a portable lidar sensor for spatially distributed snow height monitoring. Detailed water balance and karst water discharge studies at the Partnach spring investigated runoff responses to rainfall and snowmelt dynamics and characterised the karst groundwater aquifer (Hürkamp et al., 2019; Morche and Schmidt, 2012; Rappl et al., 2010; Wetzel, 2004). Numerous snow–hydrological studies investigated the spatiotemporal dynamics of snow cover and the snow water equivalent (SWE; Bernhardt et al., 2018), combining monitoring techniques, such as terrestrial photogrammetry (Härer et al., 2013, 2016), remote sensing (Härer et al., 2018) or lidar observations (Weber et al., 2016, 2020, 2021) with different complex snow–hydrological modelling. Some limitations

arising from these studies were the small number of cloud-free remote sensing scenes in the visible and near-infrared spectrum to derive spatially distributed snow cover maps at high temporal resolutions and the limited spatial extent of the terrestrial photogrammetry and lidar observations in the RCZ (Härer et al., 2016; Weber et al., 2016, 2020). Both photogrammetry and lidar observation techniques are only capable of measuring snow heights, but not hydrologically relevant SWE values, directly and thus rely on additional snow density data from local snow pit or snow weight measurements. While snow cover and snow height data are able to condition the snow–hydrological model behaviour to some degree (Weber et al., 2021), it was recently shown that integral data from satellite (Bahrami et al., 2020) and terrestrial gravimetry (Güntner et al., 2017) providing a footprint-averaged time series of the terrestrial water storage anomaly (TWSA) can greatly improve the identification of water balance components and relevant hydrological processes on catchment scale.

The last few years of terrestrial gravimetric research have seen a transformation of superconducting gravimeter (SG) installations from low noise sites for the analysis of global geophysical phenomena to specific sites of interest for the monitoring of near-surface mass transport processes. These include the development of SGs as hydrological sensors for the direct, integral and non-invasive monitoring of water storage variations in a minimised field enclosure near Tucson, Arizona, USA (Kennedy et al., 2014), and at Wettzell, Germany (Güntner et al., 2017), as well as SG installations for the monitoring of karst hydrological processes at the Larzac plateau, France (Fores et al., 2017), and at Rochefort, Belgium (Watlet et al., 2020). Creutzfeldt et al. (2013) used SG measurements at Wettzell, Germany, for the estimation of storage–discharge relationships in a small headwater catchment. Very recently, Chaffaut et al. (2021) reported about an SG installation at the summit of the Strengbach catchment in the French Vosges mountains for the analysis of water storage dynamics. In this catchment, however, seasonal snow cover only plays a minor role. In addition, SGs are applied in connection with absolute gravimeters (AGs) and relative spring gravimeters (RGs) in hybrid approaches for hydro-gravimetry (Naujoks et al., 2010), volcano monitoring (Carbone et al., 2019) and geothermal mass movements (Schäfer et al., 2020). These hybrid approaches exploit the advantages of the various types of gravimeters, with AGs providing long-term gravity changes, SGs the continuous high-precision temporal gravity changes at the measurement sites and RGs the additional spatiotemporal variations in the area of interest (Hinderer et al., 2015).

Gravimetric methods are already applied in the RCZ. Episodic AG observations were carried out since 2004 with a FG5 absolute gravimeters by the Leibniz University Hannover (LUH) for the analysis of long-term gravity changes at Mount Zugspitze and for a long-range gravimeter calibration base (Timmen et al., 2006; Peters et al., 2009). Timmen et

al. (2021) estimated a geophysical trend of  $-20 \text{ nm s}^{-2} \text{ yr}^{-1}$ , with an uncertainty of  $3 \text{ nm s}^{-2} \text{ yr}^{-1}$  (single standard deviation  $1\sigma$ ) from AG observations between 2004 and 2019 as a consequence of alpine mountain uplift and hydrological mass loss. Monthly RG observations have been done with a transportable spring gravimeter since 2014 by the Technical University of Munich (TUM) in attempt to analyse periodic permafrost changes and detect cavities in a tunnel (Kammstollen) of Mount Zugspitze (Scandroglio et al., 2019). The most important gap in the hybrid gravimetric approach was closed by the installation of the SG at the summit of Mount Zugspitze, enabling the separation of short-term, seasonal, interannual and long-term gravity changes.

In this study, we discuss to what extent the OSG 052 can contribute to a better understanding of hydrological processes in high alpine catchments. This addresses the benefits and improvements of the hydro-gravimetric approach but also its challenges and limitations. After a presentation of the available data sets from gravimetry to hydrology and meteorology in the RCZ (Sect. 2), the applied gravimetric methods for the separation of the hydrological signal from the gravity observations are shown (Sect. 3). Section 4 contains the hydro-gravimetric results and sensitivity analysis with regard to various water storage components. Section 5 summarises the main results and provides an outlook on future hydro-gravimetric projects.

## 2 Observations

### 2.1 The Zugspitze Geodynamic Observatory Germany

The Zugspitze Geodynamic Observatory Germany (ZUGOG) was set up by the German Research Centre for Geosciences (GFZ) at the summit of Mount Zugspitze, Germany's highest mountain, with an altitude of 2962 m, in a former laboratory of the Max Planck Institute for Extraterrestrial Physics (MPE) built in 1963 for the observation of cosmic rays (Fig. 2). The 10 m high tower-like aluminium structure of the lab, with an area of approx.  $50 \text{ m}^2$ , has a very steep roof to keep it free from snow. In addition, the position at the summit prevents hydrological mass variations above the sensor and simultaneously increases the hydro-gravimetric footprint (see also Chaffaut et al., 2021). Inside the lab, there is a room with two concrete piers on the ground floor. While the first concrete pier is occupied by the SG, the second one is intended for absolute and relative gravimeters, as well as other instruments. On the first floor are basic sleeping facilities for overnight stays, if necessary. A ventilation system reduces the heat produced by the compressor of the SG. This is necessary as the lab itself heats up considerably during sunny days. In addition, a thermally insulated box around the SG includes heaters to keep the sensor at a stable ambient temperature of around  $25^\circ\text{C}$  ( $\pm 1^\circ\text{C}$ ). Temperature and humidity sensors were installed in the lab. AC (mains) power is

available throughout the lab. The power supplies of all electronics and compressor are secured by uninterruptible power supplies (UPSs). The lab is accessible all year round with cable cars from Germany and Austria. The UFS provides personnel and technical support, as well as infrastructure during maintenance trips.

In September 2017, the OSG 052 was warmed up to room temperature at its former location in Sutherland, South Africa, and sent to the manufacturer GWR Instruments, Inc. in San Diego for maintenance after observing in parallel with the dual sphere OSG D-037 between 2008 and 2017 (Förste et al., 2016). This included refurbishment of the thermal levellers, an upgrade of the electronics from version GEP-2 to GEP-3, a modification of the dewar to enable cooling from room temperature down to 4 K with the accompanying refrigeration system, a replacement of the GPS antenna and a barometer specifically calibrated for a working altitude of 3000 m, as well as an Intel mini personal computer for the operation of the UIPC (User Interface PC software; GWR) software with Windows 7. After returning to GFZ, the OSG 052 was moved to ZUGOG in September 2018 by truck, cog-wheel train and helicopter at operating temperatures of 4 K. The first weeks of gravity observations with the OSG 052 showed an instrumental malfunction, with a very large negative drift of about  $-50 \text{ nm s}^{-2} \text{ d}^{-1}$  and several small offsets (cf. Schäfer et al., 2020). At the end of October 2018, the instrument was warmed then re-cooled. The manufacturer (GWR) now recommends that SGs be transported at room temperature and the dewar be evacuated just prior to cooling with the refrigeration system. According to GWR, development is currently in progress to eliminate these requirements.

The OSG 052 has been in nominal operation since 29 December 2018. ZUGOG participates in the International Geodynamics and Earth Tide Service (IGETS; Boy et al., 2020), providing level 1 raw gravity and atmospheric pressure data with sampling rates of 1 s and 1 min (Voigt et al., 2019) on a regular basis to the publicly accessible IGETS database hosted by GFZ (Voigt et al., 2016a). Absolute gravity values from FG5X-220 measurements by LUH at ZUGOG can be found in the Absolute Gravity Database (AGrav) hosted by International Gravimetric Bureau (BGI) and the German Federal Agency for Cartography and Geodesy (BKG; Wilmes et al., 2009). In addition, the continuous Global Navigation Satellite Systems (GNSS) station ZUGG nearby ZUGOG (Ramatschi et al., 2019) has been in operation since 9 September 2018 nearby the lab for the monitoring of surface displacements (Fig. 2a). Several environmental sensors monitor local hydrological and meteorological variations. A snow scale and three laser-based snow height sensors quantify the accumulated snow masses on the horizontal plane in front of the lab during the winter months (Fig. 2c). After the experiences from the first winter 2018–2019, the pole with the snow height sensors had to be extended from 2.5 to 4 m. Another laser-based snow height sensor has a view to the slope directly below the SG. Laser-based sensors were pre-

ferred instead of the widely used ultrasonic sensors because the snow cover is not horizontal. A small meteorological station outside the lab observes temperature and humidity, as well as wind speed and direction. All data sets are part of a remotely controlled monitoring system.

## 2.2 Hydrological and meteorological data sets in the research catchment Zugspitze

ZUGOG has been connected to the UFS as the home base of a large research consortium operating a dense hydrological and meteorological sensor network for more than 20 years. Long-term meteorological data sets from 1900 are available on an hourly to yearly basis from the Climate Data Center (CDC) of DWD for the station at the summit of Mount Zugspitze (station ID 5792), including relative humidity, air temperature, precipitation height and form, wind speed and direction and air pressure. LWD provides several hydrological and meteorological data sets from a station at the Zugspitzplatt at an altitude of 2420 m, including the SWE of the snowpack recorded by a snow scale. Moreover, in the last few years, three further meteorological stations were set up at the Zugspitzplatt and on two mountain ridges in the frame of the Virtual Alpine Observatory (VAO) project.

Augsburg University operates the gauge stations at Partnach spring and Bockhütte for discharge monitoring (Fig. 1), while another gauge station is planned for the Hammersbach catchment. However, massive snowfall and corresponding spring discharge in spring 2019 severely damaged the gauge station at Partnach spring and the data for the year 2019 are completely missing. A workaround was installed in the spring of 2020, and a comprehensive maintenance of the whole station is scheduled for the summer of 2021. Glaciologists of the Bavarian Academy of Sciences and Humanities have mapped the glacier areas and volumes since the 1960s (Timmen et al., 2021, Mayer et al., 2021, Hagg et al., 2012). Since 2007, the Bavarian Environmental Agency has permanently monitored the permafrost degradation within Mount Zugspitze in a borehole equipped with temperature sensors (Gallemann et al., 2017, 2021).

The data sets are compiled in the Alpine Environmental Data Analysis Center (AlpEnDAC) as part of the VAO. Overall, this high alpine region has one of the highest densities of meteorological stations worldwide and serves therefore as an ideal reference for testing new measurement and modelling approaches.

## 3 Gravimetric methodology

### 3.1 Pre-processing and calibration

The essential prerequisite for the application of the OSG 052 as a hydrological sensor is the separation of the hydrological signal from raw gravity observations. The required steps are explained for the period from 29 December 2018



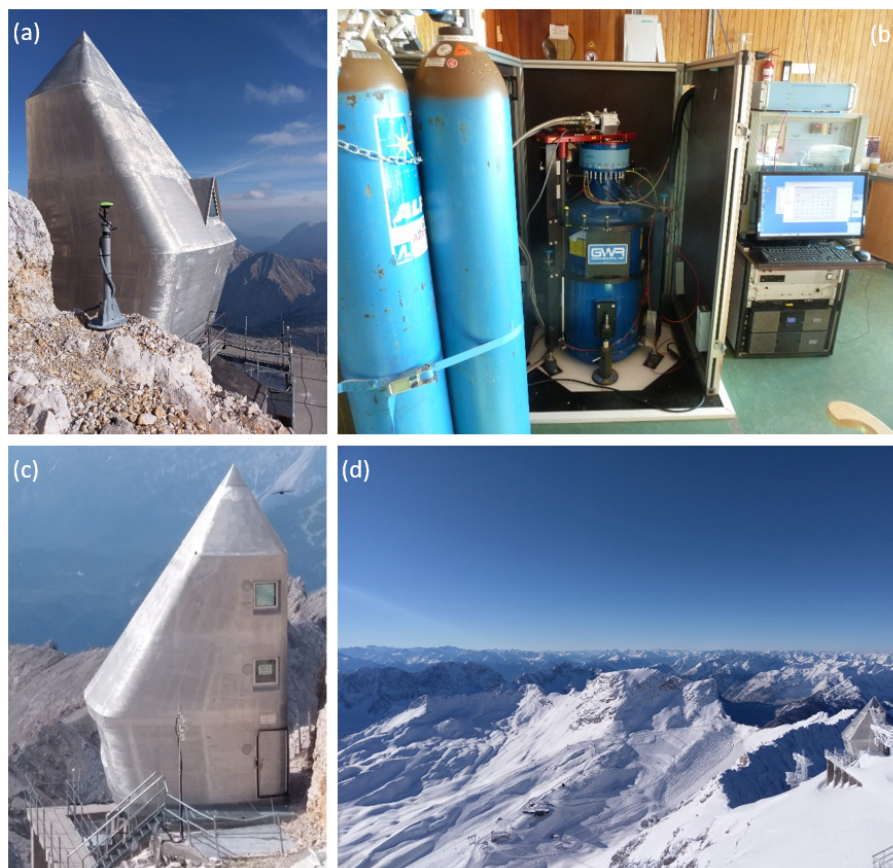


**Figure 2.** (a) The Zugspitze Geodynamic Observatory Germany (ZUGOG) with Global Navigation Satellite Systems (GNSS) station in front. (b) OSG 052 installed on the ground floor at ZUGOG. (c) ZUGOG with snow height sensors and snow scale in front. (d) ZUGOG with a winter view of a part of the alpine research catchment Zugspitze including the northern and southern Schneeferner glaciers.

to 31 March 2021 (27 months of observation). Raw gravity observations are voltage variations in 1 s sampling, along with the observed barometric pressure variations and stored in daily files of the Tsoft format (Van Camp et al., 2005). These are compiled into monthly files and converted into the GGP file format of IGETS (Voigt et al., 2016a). For the decimation from 1 s to 1 min sampling, a double precision Chebyshev filter “g1s1m”, with a filter length of 1009 s, is applied (Crossley, 2010). For the reduction of the gravity data and the removal of spikes and offsets, as well as the filling of longer gaps, the programmes DETIDE and DESPIKE of ETERNA 3.4 (Wenzel, 1997) are used. Besides some steps on 7 January 2019 during the final centring of the sphere, the time series showed only two additional steps, on 24 October 2019 during a power failure due to UPS testing and on 7 December 2020 after exchanging the CMOS battery on the GEP remote card, which are eliminated manually with the programme Tsoft. Finally, the monthly files in 1 min sampling are further decimated to one long time series in 1 h sampling by the programme DECIMATE, using symmetrical numer-

ical FIR low-pass filters “N2H1M001” and “N14H5M01” from ETERNA 3.4.

For the transition from voltage to gravity variations, the amplitude factor of the OSG 052 is estimated on the basis of two absolute gravimeters and one calibrated spring gravimeter (Table 1). The first estimation was done in 2011 at Sutherland with FG5-301 by BKG. In order to validate this result after repeated transport of the SG and refurbishment at GWR, the second estimation was done in September 2018 at ZUGOG with FG5X-220 by LUH (Timmen et al., 2021); however, it was done with a reduced accuracy due to the malfunction of the SG at this time (see Sect. 2.1). Hence, a third estimation was carried out over 4 weeks in September and October 2019 at ZUGOG on the basis of the relative spring gravimeter CG6-69 of GFZ calibrated in the gravimeter calibration system of Hannover (Timmen et al., 2020). Within a least squares adjustment, the amplitude factor of OSG 052 and a best-fitting polynomial reflecting the irregular drift of the CG6 are determined. The best-fitting solution (smallest standard deviation for the amplitude factor) is found for blocks of 3 d, polynomials of degree 3, and 50 % overlap of

**Table 1.** Amplitude factors of the OSG 052 estimated from three calibrations.

| No. of calibration | Method         | Site       | Period             | Amplitude factor<br>(nm s <sup>−2</sup> V <sup>−1</sup> ) | 1σ uncertainty<br>(nm s <sup>−2</sup> V <sup>−1</sup> ) |
|--------------------|----------------|------------|--------------------|---|---|
| 1                  | FG5-301 (BKG)  | Sutherland | 23–26 Nov 2011     | −748.3  | 0.5   |
| 2                  | FG5X-220 (LUH) | Zugspitze  | 15–20 Oct 2018     | −746.68   | 1.30  |
| 3                  | CG6-69 (GFZ)   | Zugspitze  | 27 Sep–24 Oct 2019 | −750.03   | 0.25  |
| Mean value         |                |            |                    | −749.59   | 0.22  |

the blocks. The final amplitude factor is  $-749.59 \text{ nm s}^{-2} \text{ V}^{-1}$  ( $1\sigma = 0.22 \text{ nm s}^{-2} \text{ V}^{-1}$ ) as a weighted mean from calibrations 1–3. The achieved accuracy is sufficient with regard to gravity residuals with a range of  $750 \text{ nm s}^{-2}$  (Fig. 3g), as amplitude factor deviations of  $1 \text{ nm s}^{-2} \text{ V}^{-1}$  correspond to maximum deviations of  $1 \text{ nm s}^{-2}$  in gravity residuals, which represents a conservative estimate of the accuracy of the gravity observations at ZUGOG.

The time delay of the OSG 052 is determined within a step response experiment developed by GWR on 1 March 2019 at ZUGOG. In total, 16 introduced step voltages are analysed with the programme ETSTEP of ETERNA 3.4 (Wenzel, 1997), and the time delay is estimated to 10.53 s ( $1\sigma = 0.03 \text{ s}$ ).

The instrumental drift of the OSG 052 is estimated to be  $-20 \text{ nm s}^{-2} \text{ yr}^{-1}$  based on two absolute measurements with FG5X-220 by LUH at 26–27 September 2019 and 30–31 March 2021 with 2477 and 5166 drops, respectively (Fig. 3g). With regard to the uncertainty of  $10\text{--}20 \text{ nm s}^{-2}$  ( $1\sigma$ ) for the absolute measurements and the knowledge that the SG drift is small and linear towards increasing gravity, the null hypothesis for the drift cannot be disproved statistically, and no drift is applied within the subsequent analysis. Further absolute measurements planned for the future will increase the redundancy of the drift estimation and longer temporal differences between the absolute measurements will make the drift estimation more robust. Unfortunately, the first absolute measurements from 15–20 October 2018 cannot be used as additional reference value for the drift estimation, as the SG had to be warmed up and cooled again for re-initialisation at the end of December 2018 (Sect. 2.1) so that there is no connection to the current continuous SG time series.

3.2 Tidal analysis

In order to reduce the gravity effects from solid Earth and ocean tides, a local tidal model is computed based on 2 years of observations (29 December 2018–31 December 2020) with the programme ANALYZE of ETERNA 3.4 (Wenzel, 1997) for the analysis of monthly, diurnal, semidiurnal and shorter tidal waves. The estimated amplitude factors and phase leads according to the ETERNA wave grouping for a 1 year gravity time series are displayed in Table 2. The numerical high-pass filtering and a Hann win-

dow usually applied for the analysis of diurnal and semi-diurnal waves are deactivated for the simultaneous analysis of the monthly waves, resulting in higher standard deviations for the shorter waves. Instead, a Chebyshev polynomial of degree 2 is applied in order to eliminate any long-term instrumental trend signal or long-term variations in gravity. Longer tidal waves (half-year periods and longer) are considered by nominal values, i.e. amplitude factors of 1.16 and phases of  $0^\circ$ . Along with the tidal waves, the single admittance factor between gravity and barometric pressure is determined with  $-3.65 \text{ nm s}^{-2} \text{ hPa}^{-1}$  ( $1\sigma = 0.04 \text{ nm s}^{-2} \text{ hPa}^{-1}$ ). In order to reduce the large seasonal gravity signal, a second admittance factor is determined between gravity and the snow water equivalent (SWE), with  $0.2965 \text{ nm s}^{-2} \text{ mm}^{-1}$  ( $1\sigma = 0.0007 \text{ nm s}^{-2} \text{ mm}^{-1}$ ; cf. Sect. 4.2). The gravity variations induced by solid Earth and ocean tides are predicted with the local tidal parameters from Table 2 and are shown for the analysed period in Fig. 3b.

3.3 Non-tidal gravity reductions

Besides tidal variations, the gravity observations include significant non-tidal effects (shown in Fig. 3). For a more detailed compilation of temporal gravity field variations see, e.g., Voigt et al. (2016b), while Mikolaj et al. (2019) quantify time domain uncertainties for the different gravity reductions. The signal admittance factor of  $-3.65 \text{ nm s}^{-2} \text{ hPa}^{-1}$ , estimated together with the tidal analysis, includes the maximum correlated signal between observed gravity and barometric pressure. For a refined modelling of gravity variations induced by mass redistributions in the atmosphere, the Atmospheric Attraction Computation Service (ATMACS; Klügel and Wziontek, 2009) provides effects from local to global scales, with a temporal resolution of 3 h based on 3D ECMWF (European Centre for Medium-Range Weather Forecasts) weather data. However, the limited spatial resolution of the weather models of 7 km for Europe shows that the complex topography around the station cannot be represented sufficiently. In order to account for the limited spatial resolution and to improve the temporal resolution, the following procedure is used. The gravity observations are reduced by the effects of solid Earth and ocean tides, Earth rotation and SWE variations, as well as regional and global atmospheric effects from ATMACS. In this way, the

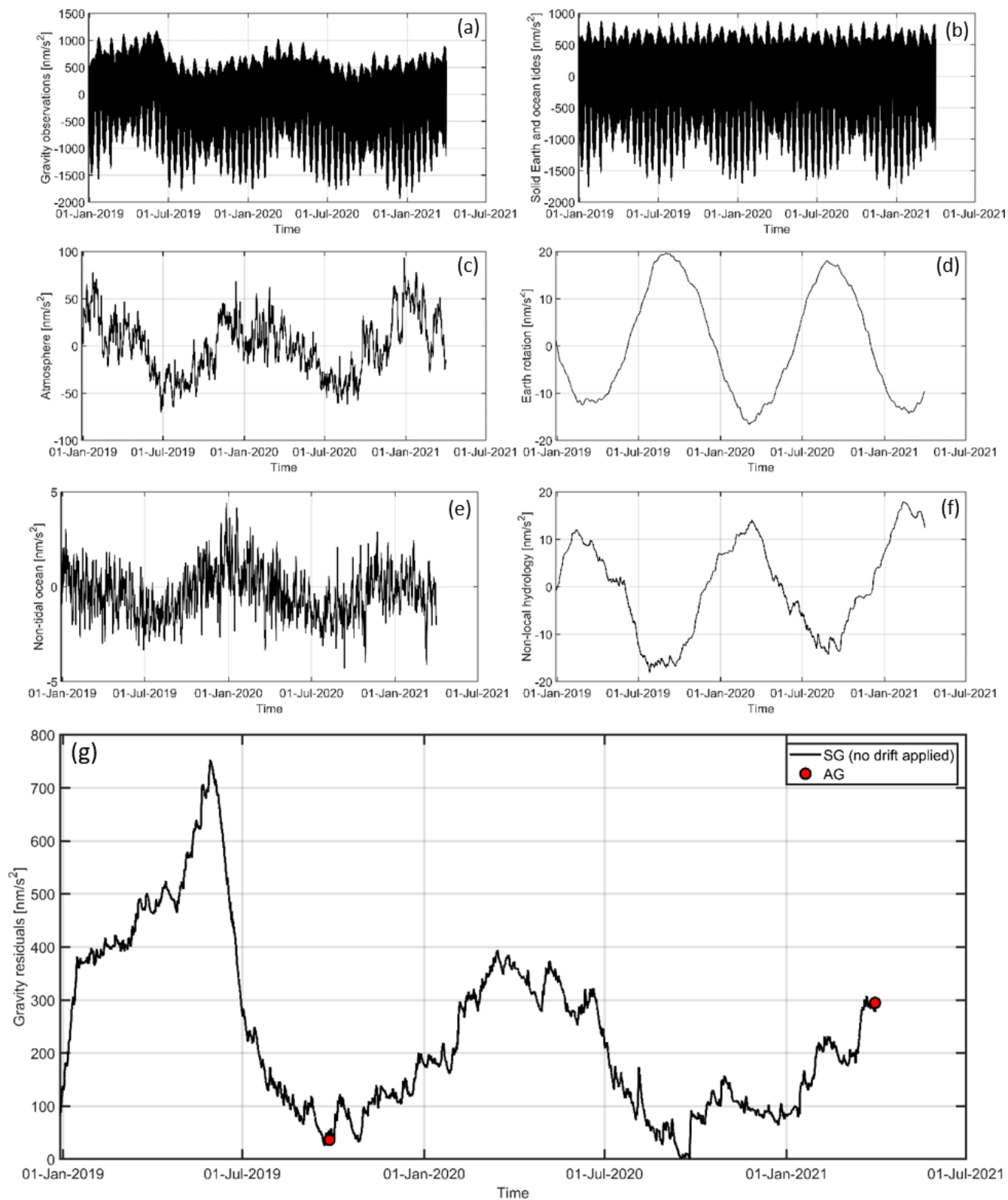


**Figure 3.** Signal separation from gravity observations (a) to gravity residuals (g), including two absolute measurements (red circles) by reducing gravity variations induced by solid Earth and ocean tides (b), atmospheric mass redistributions (c), Earth rotation (d), non-tidal ocean (e) and non-local hydrological mass redistributions (f). Please note the different scaling of the axes.

**Table 2.** Estimated amplitude factors and phase leads from a least squares adjustment of 23 tidal waves based on 2 years of gravity observations with OSG 052 at ZUGOG.

| Frequencies (cpd) |          | Wave | Theoretical<br>amp. ( $\text{nm s}^{-2}$ ) | Amplitude<br>factor | Std      | Phase lead<br>( $^{\circ}$ ) | Std<br>( $^{\circ}$ ) |
|-------------------|----------|------|--|---------------------|----------|------------------------------|-----------------------|
| From              | To       |      |  |                     |          |                              |                       |
| 0.020885          | 0.054747 | MM   | 21.1656                                    | 1.01201             | 0.18789  | 9.1622                       | 10.6146               |
| 0.054748          | 0.091348 | MF   | 40.0581                                    | 1.11718             | 0.04843  | 5.8775                       | 2.4845                |
| 0.091349          | 0.122801 | MTM  | 7.6699                                     | 1.42938             | 0.16566  | −6.1562                      | 6.6347                |
| 0.122802          | 0.501369 | MQM  | 1.2250                                     | 1.24028             | 0.60193  | 5.1859                       | 27.8178               |
| 0.501370          | 0.911390 | Q1   | 59.3059                                    | 1.14954             | 0.00152  | −0.1425                      | 0.0756                |
| 0.911391          | 0.947991 | O1   | 309.7475                                   | 1.15060             | 0.00031  | 0.0454                       | 0.0154                |
| 0.947992          | 0.981854 | NO1  | 24.3484                                    | 1.14980             | 0.00302  | 0.3313                       | 0.1505                |
| 0.981855          | 0.998631 | P1   | 144.1019                                   | 1.15094             | 0.00066  | 0.0240                       | 0.0327                |
| 0.998632          | 1.001369 | S1   | 3.4048                                     | 1.38514             | 0.03875  | 23.9574                      | 1.6028                |
| 1.001370          | 1.023622 | K1   | 435.4574                                   | 1.13835             | 0.00022  | 0.1490                       | 0.0110                |
| 1.023623          | 1.035379 | TET1 | 4.6578                                     | 1.15618             | 0.02065  | 1.1388                       | 1.0233                |
| 1.035380          | 1.057485 | J1   | 24.3569                                    | 1.15438             | 0.00384  | 0.0779                       | 0.1905                |
| 1.057486          | 1.071833 | SO1  | 4.0394                                     | 1.13676             | 0.02372  | 0.9770                       | 1.1951                |
| 1.071834          | 1.470243 | OO1  | 13.3201                                    | 1.15354             | 0.00642  | 0.1334                       | 0.3188                |
| 1.470244          | 1.880264 | 2N2  | 10.5279                                    | 1.15943             | 0.00249  | 2.4868                       | 0.1229                |
| 1.880265          | 1.914128 | N2   | 65.9181                                    | 1.17379             | 0.00053  | 2.0941                       | 0.0260                |
| 1.914129          | 1.950419 | M2   | 344.2804                                   | 1.18640             | 0.00011  | 1.5090                       | 0.0052                |
| 1.950420          | 1.984282 | L2   | 9.7321                                     | 1.17467             | 0.00407  | 1.7836                       | 0.1984                |
| 1.984283          | 2.002736 | S2   | 160.1632                                   | 1.18501             | 0.00023  | 0.1346                       | 0.0112                |
| 2.002737          | 2.451943 | K2   | 43.5108                                    | 1.18753             | 0.00087  | 0.4461                       | 0.0422                |
| 2.451944          | 3.381378 | M3   | 4.5825                                     | 1.07740             | 0.00484  | −0.0481                      | 0.2573                |
| 3.381379          | 4.347615 | M4   | 0.0566                                     | 0.25408             | 0.25504  | 95.3389                      | 57.5061               |
| 4.347616          | 7.000000 | M5   | 0.0007                                     | 29.93575            | 20.46948 | 30.4792                      | 39.1786               |

gravity residuals primarily reflect the effects of local atmospheric mass redistributions. The admittance factor between these gravity residuals and the observed barometric pressure variations are estimated to be  $-2.92 \text{ nm s}^{-2} \text{ hPa}^{-1}$  ( $1\sigma = 0.03 \text{ nm s}^{-2} \text{ hPa}^{-1}$ ). For the total atmospheric reduction, the local part of ATMACS is replaced by this admittance factor multiplied by the observed pressure variations in 1 h sampling and added to the regional and global atmospheric effects from ATMACS (Fig. 3c).

Temporal variations of the Earth's rotation vector with respect to the Earth's body are described by the pole coordinates and the Earth rotation angle and provided as Earth Orientation Parameters (EOPs) by the International Earth Rotation and Reference Systems Service (IERS). For the computation of the thereby induced gravity variations, the programme PREDICT of ETERNA 3.4 (Wenzel, 1997) is applied with the long-term file EOP 14 C04 (IAU1980) provided by IERS, and the amplitude factors are set to 1.16, considering the elastic properties of a deformable solid Earth (Fig. 3d).

Non-tidal ocean loading at Mount Zugspitze is caused by the attraction of non-tidal water mass variations in the Atlantic Ocean and the Mediterranean Sea and the vertical displacement of the Earth's crust due to the loading of these water masses. For the computation of these small effects with a range of  $5 \text{ nm s}^{-2}$ , the MATLAB toolbox mGlobe

v1.1.0 (Mikolaj et al., 2016) is applied on the basis of 3 h total ocean bottom pressure anomalies (data set “oba”) from the GRACE Atmosphere and Ocean De-Aliasing Level-1B (AOD1B RL06) products (Dobslaw et al., 2017) and is shown in Fig. 3e.

Hydrological gravity variations can be subdivided into those from local scales (up to several metres around the gravimeter) over alpine catchment scales (from several metres to kilometres) to non-local scales (from several kilometres). Non-local hydrological gravity variations include both attraction effects and surface loading, while for local to catchment scales only the attraction effects from mass redistributions are considered. Non-local hydrological effects are provided by the EOST loading service (Boy, 2021) using, e.g. the Modern-Era Retrospective analysis for Research and Applications, version 2 (MERRA-2; Gelaro et al., 2017), with spatial resolutions of 0.5 and  $0.625^{\circ}$  in latitude and longitude, respectively, and 1 h temporal resampling. These effects are displayed in Fig. 3f.

Figure 3 shows the process of signal separation from gravity observations of OSG 052 to gravity residuals by reducing all shown and explained effects for the period from 29 December 2018 to 31 March 2021. These gravity residuals are the primary target signal for hydro-gravimetric studies at Mount Zugspitze reflecting predominantly total water storage variations on different scales. An exceptionally



large seasonal gravity range of up to  $750 \text{ nm s}^{-2}$  is visible compared to other SG installations in Central Europe, with seasonal variations of approx.  $100 \text{ nm s}^{-2}$  range (Abe et al., 2012). However, the gravity residuals include uncertainties in the model-based signal separation, which are typically at the level of a few nanometers per second squared (hereafter  $\text{nm s}^{-2}$ ) root mean square error (Mikolaj et al., 2019). In addition, non-hydrological signals from alpine geological mass redistributions are also included in the gravity residuals. Typical examples are avalanches, rockfalls and landslides occurring on timescales from seconds to days. Regular controlled avalanche blasting with an impact of approx.  $-5 \text{ nm s}^{-2}$  on the gravity signal have already been noticed. On long timescales, the impact of mountain uplift and its separation from climate-driven long-term hydrological variations must be considered (Timmen et al., 2021).

An important task is the reduction of local hydrological signals in order to enhance the sensitivity towards the catchment scale. While the steep roof of the lab and its position above the slope at the summit are very advantageous, most of the disturbing signals are expected from snow masses on a horizontal plane with an area of  $5 \text{ m} \times 10 \text{ m}$  directly in front of the lab (Fig. 2c) where a local snow monitoring network was set up. Here, considerable amounts of snow accumulate during the winter due to precipitation, drift of snow and snow cleared off a nearby visitors' platform with a snow blower. An estimation of the maximum signal from snow heights of  $4 \text{ m}$  and densities of  $300 \text{ kg m}^{-3}$  reveals a significant gravity effect of  $25 \text{ nm s}^{-2}$  superimposed by somewhat smaller event-like signals during heavy snowfall events. As this is only a fraction of 1 : 30 with regard to the total gravity residual range and due to initial problems as a consequence of very harsh conditions during winter 2018–2019 (frozen snow height sensors, torn cables and too low sensor pole height), a model-based description of the local snowpack situation has not yet been set up completely.

## 4 Hydro-gravimetric results and sensitivity analysis

### 4.1 Water balance

The subsequent hydro-gravimetric analysis based on the gravity residuals from Fig. 3g focus, for the first time, on a high alpine region largely dominated by seasonal snow cover. The gravity residuals reflect the total water storage variations from local to catchment scales as the balance of precipitation, glacial melt, retention in the karst, spring discharge and evapotranspiration. While the large complexity and variability in the hydrological parameters make the hydrological modelling very difficult, continuous gravity observations are integrative and are thus highly beneficial, serving as constraints for the hydrological modelling on catchment scale.

From the first 27 months of observations, the high interannual variability in water storage maxima amounts to  $752 \text{ nm s}^{-2}$  at 29 May 2019 and  $393 \text{ nm s}^{-2}$  at 14 March 2020, significantly differing according to the time of year and in amplitude by a factor of 2 due to seasonal snowpack variations. The seasonal minima, however, are very close in time and amplitude, with a difference of  $-24 \text{ nm s}^{-2}$  between 16 September 2020 and 21 September 2019, respectively, agreeing with the trend of  $-20 \text{ nm s}^{-2} \text{ yr}^{-1}$  estimated from absolute gravity observations between 2004 and 2019 by Timmen et al. (2021). They suggest that the main contribution is caused by glacier diminishing, and a smaller part is explained by mountain uplift ( $1 \text{ mm}$  causes  $-2 \text{ nm s}^{-2}$ ). With a multi-year continuous gravity time series from OSG 052, it is possible to study the evolution of seasonal and – in combination with absolute gravity observations – also long-term water storage variations.

For the hydrological decomposition of the gravity residuals into individual water storage components, complementary data from meteorological and hydrological techniques are needed. According to Newton's law of gravitation, the gravimetric method is known to be most sensitive to local mass variations with a signal attenuation by  $1/r^2$  ( $r$  being the distance between gravimeter and source mass). As gravimeters are solely sensitive in a vertical direction, attenuations occur for mass variations towards the horizontal direction (see also Creutzfeldt et al., 2008). Hence, the essential question is how sensitive the gravity residuals are with regard to individual water storage components from local to catchment scales. This question will be addressed in the following sections.

### 4.2 Snowpack

Representative observations of the snow water equivalent (SWE) for the Zugspitzplatt are available from the LWD station (Fig. 1). The spatiotemporal variations in the snowpack around the summit of Mount Zugspitze are the main contributors to the gravity residuals from autumn to spring. Figure 4 shows the gravity residuals, the SWE multiplied by the estimated regression factor between gravity residuals and SWE of  $0.298 \text{ nm s}^{-2} \text{ mm}^{-1}$  ( $1\sigma = 0.003 \text{ nm s}^{-2} \text{ mm}^{-1}$ ). The high correlation of 0.963 between the gravity residuals and SWE (sample size 19 771) is clearly visible, and both follow similar seasonal patterns.

In general, the winter seasons of 2018–2019 and 2019–2020 were very different. The first winter season is characterised by a sharp increase in SWE of approx.  $300 \text{ nm s}^{-2}$  in mid-January and in the second half of May due to massive snowfall. The maximum SWE is extraordinarily high, with a value of  $1957 \text{ mm}$  measured at the LWD station, compared to an annual mean of the maximum SWE at approx.  $1350 \text{ mm}$  since the installation of the snow scale in 2014. On the contrary, the second winter season with a maximum SWE of  $1147 \text{ mm}$  at the LWD station represents a winter

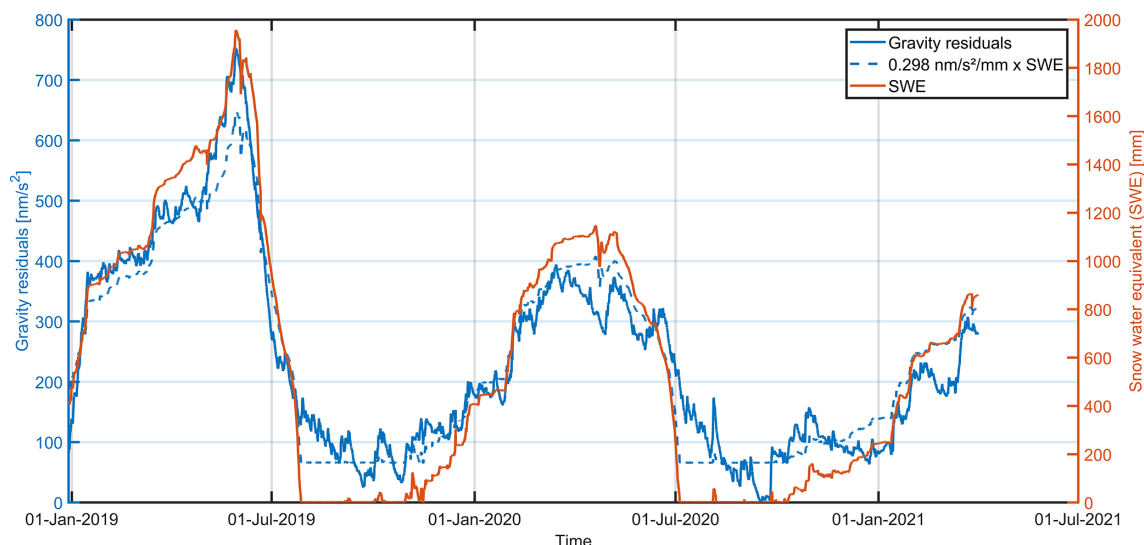


**Figure 4.** Gravity residuals (solid blue), snow water equivalent (solid red) from LWD station at Zugspitzplatt and SWE multiplied with the estimated regression factor of  $0.298 \text{ nm s}^{-2} \text{ mm}^{-1}$  between gravity residuals and snow water equivalent (dashed blue line).

with a small to normal amount of snow. While in 2019 the seasonal gravity and SWE maxima coincide at 29 May, there is a difference of more than 1 month between gravity and SWE maxima in 2020, i.e. 14 March and 19 April, respectively. However, in 2020 there was no distinctive SWE peak but rather a longer period with SWE values near maximum between these two dates. Higher temperatures in April 2020 led to an early onset of snowmelt in the lower part of the catchment, with recharge of the karst water body beginning and increasing spring discharge at Partnach spring.

Besides the high correlation between gravity and SWE from the LWD station at Zugspitzplatt, there are still significant additional signals remaining with a range of  $250 \text{ nm s}^{-2}$  in the differences between gravity residuals and  $0.298 \text{ nm s}^{-2} \text{ mm}^{-1} \times \text{SWE}$  (Fig. 4). The reasons are manifold. First, the single point observations of the SWE at LWD station are not fully representative of the large variations in the SWE and its distribution at catchment scale, particularly considering the altitude and temperature gradient within the area. During periods of massive snowfall, e.g. from 29 December 2018 to mid-January 2019, this leads to remaining signals of up to  $150 \text{ nm s}^{-2}$ . Second, signals from other water storage components are not considered within the regression analysis. Major remaining signals of up to  $200 \text{ nm s}^{-2}$  occur during the main melting periods and corresponding spring discharge from May to July (Fig. 6). Moreover, rain events during the short summer season cause rapid gravity increases of up to  $100 \text{ nm s}^{-2}$ , e.g. from 3 to 4 August 2020, followed by an equally fast but only partial decrease and a slower subsequent decline due to the lagged drainage back to the gravity level before the specific rain event (Timmen et al., 2021).

Sensitivity analysis of a simple snowpack distribution assumption in the surroundings are carried out for the times of

maximum seasonal gravity residuals on 29 May 2019 and 14 March 2020. In order to take into account the topography for the spatial snow distribution, the high-resolution digital terrain model DGM50 M745 by BKG from 2006, with a grid spacing of  $1'' \times 1''$  (long20 m  $\times$  lat30 m), is used. The following assumptions are made for the snowpack distribution at the specific dates:

1. computing the gravity effect from topography by integration of all rectangular prisms of  $20 \text{ m} \times 30 \text{ m}$  areas and constant heights;
2. putting a homogeneous snowpack of maximum SWE of 1957 and 1075 mm, respectively, on top of every rectangular prism for the topography;
3. decreasing the snowpack linearly on slopes with a value of 50 % at  $45^\circ$  slope and 0 % at  $90^\circ$  slope; and
4. decreasing the snowpack linearly even further for lower elevations between 2000 and 1500 m with 0 % snowpack at 1500 m (only valid for the late spring of the examples).

Figure 5 shows the assumed spatial distribution of the snowpack around Mount Zugspitze on 29 May 2019 and 14 March 2020 (Fig. 5a and c, respectively) and the cumulative snow–gravimetric sensitivities with regard to the ZUGOG gravimeter site (b and d, respectively) with the essential results summarised in Table 3. The assumed snow distributions provide gravity values of  $764 \text{ nm s}^{-2}$  ( $752 \text{ nm s}^{-2}$  observed) and  $420 \text{ nm s}^{-2}$  ( $393 \text{ nm s}^{-2}$  observed), respectively, for the two dates corresponding to deviations of 2 % and 6 % between assumption and observation. The gravity contributions from all areas coloured from deep red to yellow in

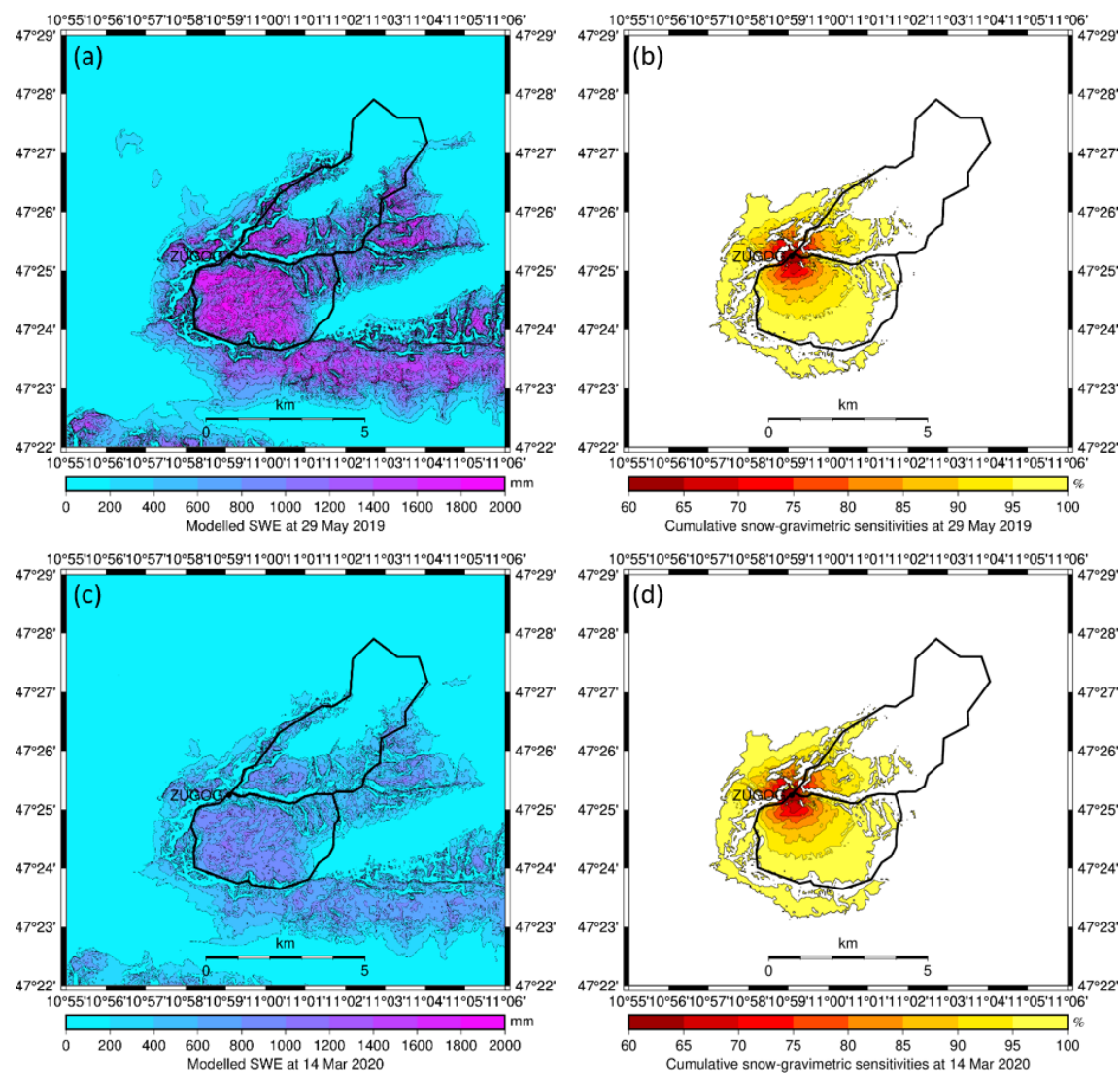


**Figure 5.** Assumed SWE of the snowpack at maximum seasonal gravity residuals **(a, c)** and corresponding cumulative snow–gravimetric sensitivities **(b, d)** with regard to ZUGOG at 29 May 2019 and 14 March 2020, respectively. The boundaries of the Partnach spring and Hammersbach catchments are shown as a black line. Sensitivities are shown only up to 99.87 % and 99.76 %, respectively, for the given examples, omitting residuals of  $1 \text{ nm s}^{-2}$  of the total signal.

**Table 3.** Gravity contributions from modelled snowpack of various areas with regard to ZUGOG at maximum seasonal gravity residuals on 29 May 2019 and 14 March 2020.

| Area  | 29 May 2019                           |                        | 14 March 2020                         |                        |
|---|---------------------------------------|------------------------|---------------------------------------|------------------------|
|   | $\Delta g \text{ (nm s}^{-2}\text{)}$ | $\Delta g \text{ (%)}$ | $\Delta g \text{ (nm s}^{-2}\text{)}$ | $\Delta g \text{ (%)}$ |
| Total   | 763.9                                 | 100.0                  | 420.4                                 | 100.0                  |
| Snow–gravimetric footprint (deep red to yellow areas in Fig. 5) | 762.9                                 | 99.9                   | 419.4                                 | 99.8                   |
| Partnach spring catchment (RCZ)                                 | 542.0                                 | 71.0                   | 297.6                                 | 70.8                   |
| Hammersbach catchment   | 46.3                                  | 6.1                    | 25.5                                  | 6.1                    |

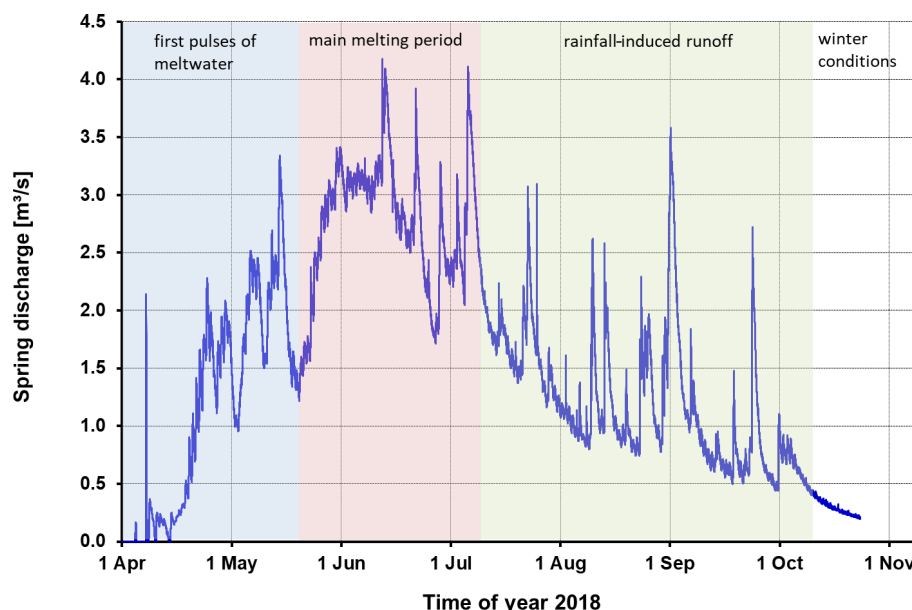


**Figure 6.** Spring discharge characteristics of the Partnach spring during 2018.

Figs. 5b and d are defined as the snow–gravimetric footprint, with contributions of 99.87 % (29 May 2019) and 99.76 % (14 March 2020), respectively. Areas contributing together a remaining gravity signal of  $1 \text{ nm s}^{-2}$  are omitted (Table 3).

The results show that the gravimeter observations are sensitive to the snowpack on catchment scales up to 3.5 km horizontal and 4 km slant distances to the gravimeter with a resulting snow–gravimetric footprint of approx.  $40 \text{ km}^2$  (Fig. 5). The major contribution comes from prisms in the RCZ with 71 % in both examples. The Hammersbach catchment has a much less significant contribution of 6 % only as this lies on the opposite side of Mount Zugspitze and has very steep slopes near the summit. The additional gravity contribution from the snowpack in the remaining eastern parts of the Bockhütte catchment is negligible. The assumed spatial distribution of the snowpack suggests that the remaining 23 % contribution to the total gravity signal come from snow masses of the nearby summit area northwest of ZUGOG. These effects in close vicinity should be much smaller in reality, compared to our very simple assumption of snow distribution, as the maximum snowpack at the summit is certainly less than the values from the LWD station due to usually strong winds at the summit ridge, which are neglected up to this point. Also the topography to the northwest of ZUGOG is very steep, in parts vertical, which allows for less snow accumulation and frequent discharge in the form of avalanches. Still, the local snowpack distribution in the direct vicinity of the SG needs special attention due to artificial snow accumulation around the summit which are monitored by a snow scale and snow height sensors (Fig. 2c). This knowledge will improve the snow–gravimetric sensitivities towards catchment scales.

### 4.3 Karst groundwater and spring discharge

Besides snow distribution and snow water equivalent, the liquid water balance in the karstified RCZ is influencing the SG signal. Throughout the year, a typical course of spring discharge with four characteristic periods can be observed at the Partnach spring gauge (Fig. 6). From the end of October to April no recharge of the karst system takes place, and the Partnach spring falls dry. With rising temperatures in April, melting processes begin in the lower parts of the catchment, and the first meltwater pulses are observed at the Partnach river gauge. A melting period in the upper part of RCZ starts later in May lasting until the beginning of July. The karst system of RCZ is mainly fed by meltwater, and discharge at the Partnach spring is continuously high. Liquid precipitation leads to pronounced spring discharge peaks on top of the increased basal discharge level. During this period of time, spring discharge at the Partnach spring is a mixture of meltwater from areas with increasing elevations and liquid precipitation. After melting ends, long lasting rainfall and storm precipitation dominate spring discharge characteristics with steep rising and falling limbs. The well-developed karst system of RCZ with conduit flow causes these rapid spring discharge reactions of the Partnach spring. With lowering temperatures during autumn, snow accumulation starts in higher elevations of RCZ, and recharge of karst groundwater is reduced because liquid precipitation is more seldom. Sometimes daily melting cycles of the glacier remains of the northern and southern Schneeferner can be observed during this usually dry period. At the end of autumn, low temperatures and snowfall in higher elevations terminate recharge

and karst groundwater head falls, step by step, beneath the level of the Partnach spring.

During seasonal snowmelt periods in spring and especially after the snowpack has fully disappeared in summer, other signals become the main contributors to the water storage variations observed by the gravimeter. The largest part of the melting snow fills the vadose zone of the karstified underground body below the Zugspitzplatt (Fig. 1). If the groundwater level is rising with beginning recharge of the vadose zone, the spring discharge starts at the Partnach spring which is usually well observed by a gauge station. However, the spring discharge data are not available for 2019 (Sect. 2.2). From the seasonal gravity minima at 21 September 2019 and 16 September 2020, respectively, being very close in time despite the very different snow masses, a large variability in the spring discharge processes as a consequence of the seasonal snowpack can be stated.

For the hydrological interpretation of gravity signals from ZUGOG, it is crucial to quantify the water volume stored in the vadose karst zone of RCZ. Thereto, pseudo-continuous depletion curves are constructed by splicing short falling hydrograph intervals together (e.g. Lamb and Beven, 1997). The recession constant “ $\alpha$ ” is calculated for several years because the recession behaviour of the Partnach spring varies from year to year due to unknown processes in the karst system (Fig. 7a). Based on a mean recession constant  $\alpha$ , a water storage model for the vadose karst zone is developed by an addition of daily discharge volumes during the depletion period. As Fig. 7b shows, storage volume in the vadose zone varies between 1.6 and  $3.38 \times 10^6 \text{ m}^3$ . Under the assumption of a homogeneous layer of a  $6 \text{ km}^2$  wide groundwater body (Fig. 1), these numbers correspond to water storage changes of 0.27 and 0.56 m, respectively, that can be translated to groundwater level changes depending on the aquifer porosity. Sensitivity analysis with regard to the ZUGOG site reveal corresponding gravity values between 12 and  $24 \text{ nm s}^{-2}$ , respectively. With an uncertainty of a few  $\text{nm s}^{-2}$ , the gravimetric approach should be able to distinguish interannual groundwater storage variations and allow for comparison with the water balance and karst water discharge studies at the Partnach spring. Besides seasonal spring discharge and corresponding karst groundwater variations, rainfall events on timescales from hours to days produce significant peak-like signals not only in the spring discharge but also in the gravimetric time series. A homogeneous layer of 1 mm precipitation height on top of the digital terrain model applied (Sect. 4.2) results in a gravity increase of  $0.9 \text{ nm s}^{-2}$ . This shows that the gravity variations can be used as reference for the estimation of the total sum of precipitation (Delobbe et al., 2019) in this alpine terrain with large variability in precipitation instead of using point measurements with precipitation collectors. The higher precipitation admittance factor (factor of 3 compared to  $0.298 \text{ nm s}^{-2} \text{ mm}^{-1}$  for the SWE) results from the large geographical heterogeneity of the SWE in the RCZ. The SWE of the snowpack recorded by the snow

scale at the LWD station provides maximum SWE values, while the precipitation height is set as a homogeneous layer.

The same hydro-gravimetric approach might be applied to the estimation of daily evapotranspiration rates (Van Camp et al., 2016) during dry days in late summer (August and September) when the seasonal spring discharge has mainly finished. In general, evapotranspiration is small in high alpine areas, especially due to less available soil moisture in shallow alpine soils or even the absence of soils at all, sparse vegetation and less demand of plants and decreases with increasing altitude (Gurtz et al., 1999). Maximum evapotranspiration rates of  $2\text{--}3 \text{ mm d}^{-1}$  for high alpine environments inducing gravity effects of 1.8 to  $2.7 \text{ nm s}^{-2}$ , respectively, at the ZUGOG gravimeter site are at the limit of what can be observed by the gravimeter.

Finally, glacier melting and permafrost degradation also contribute to groundwater and spring discharge with predominant climate-driven long-term signals but also significant interannual variations, e.g., as a consequence of very dry and hot summers (Scandroglio et al., 2019). In addition, cavities inside Mount Zugspitze filled with water through permafrost degradation might influence the gravimetric signal on a catchment scale, depending on the distance and direction to the gravimeter and their sizes. These additional signals will be best captured by the combination of absolute, superconducting and relative gravimetry and other geodetic techniques in a future hybrid approach.

## 5 Summary and conclusions

The superconducting gravimeter OSG 052 is introduced as a novel hydrological sensor for the direct observation of the integral gravity effect of total water storage variations in the high alpine Partnach spring catchment (Research Catchment Zugspitze – RCZ), and a high-quality and publicly available continuous gravity time series of 27 months is provided. The RCZ is among the best-equipped high alpine catchments with lysimeter characteristics and is now supplemented by a superconducting gravimeter to address the complex hydrological situation dominated by snow cover, melting glaciers and degrading permafrost, as well as karst groundwater.

Spatiotemporal variations in the snowpack are the main contributor to the gravity residuals. Gravity residuals from the OSG 052 and the SWE measured with a snow scale at an altitude of 2420 m are highly correlated (0.963) and reveal a regression factor of  $0.298 \text{ nm s}^{-2} \text{ mm}^{-1}$  ( $1\sigma = 0.003 \text{ nm s}^{-2} \text{ mm}^{-1}$ ). The large range of gravity residuals up to  $750 \text{ nm s}^{-2}$  corresponds to the maximum of 1957 mm snow water equivalent on 29 May 2019, measured at the LWD station located on the Zugspitzplatt. Sensitivity analysis on the basis of a simplified assumption on snow distribution in this area reveal a snow–gravimetric footprint of 3.5 km horizontal and 4 km slant distances around the gravimeter, covering an area of  $40 \text{ km}^2$ . This result, together



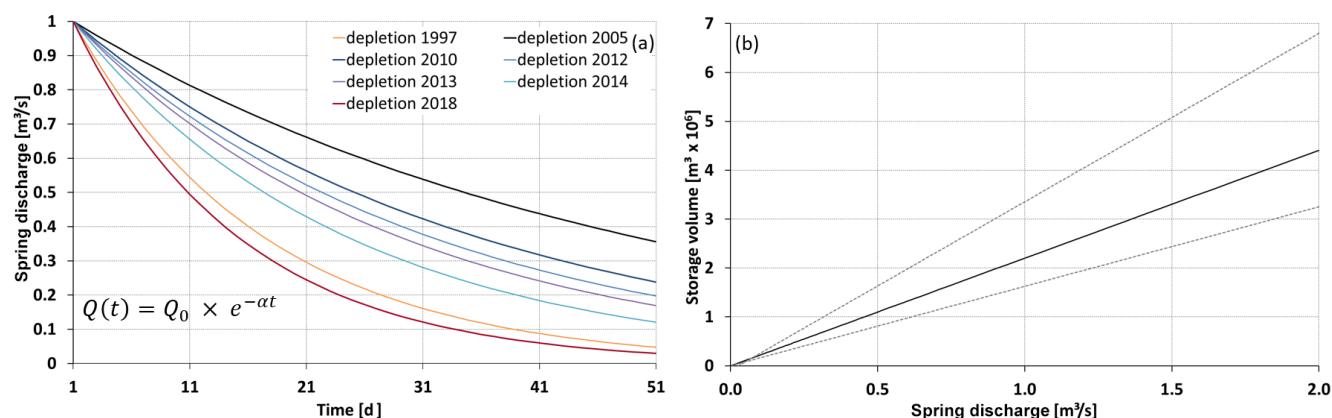


**Figure 7.** Depletion curves of the karst groundwater of RCZ for selected years (a) and calculated storage volumes of the groundwater body at different levels of spring discharge (b). The solid line shows the relationship for a mean recession constant “ $\alpha$ ” of 0.4, and the dashed lines are enclosing the range of 1 standard deviation.

with the low uncertainty of the gravity residuals of a few  $\text{nm s}^{-2}$ , enables various detailed future hydro-gravimetric analysis as the snow masses from the RCZ contribute to more than two-thirds of the total gravity signal.

Based on this concept study, it is certainly useful to also study the non-linearity of the relationship between gravity residuals and SWE, i.e. is there a significant dependence on snow height? Moreover, the description of the snowpack distribution will be refined in future studies for the entire Zugspitze region and the three catchments of Partnach spring, Bockhütte and Hammersbach. The aim is to set up snowpack models such as SNOWPACK/Alpine3D (Lehning et al., 2006) or use cold region hydrological model frames like the Canadian Hydrological Model (CHM; Marsh et al., 2020) at this location, and, in addition, to statistically describe the main snowpack distribution via lidar measurements, similar to those presented in Grünewald et al. (2013). With these approaches, the descriptions of the spatial snowpack distribution will be improved in this very complex high alpine terrain by including detailed descriptions of the snowpack itself, the effect of the energy balance on the snowpack, potential wind redistributions and further meteorological and gravimetric influences on the snow cover regarding elevation, aspect and slope and by using the gravity residuals as boundary conditions.

During the mainly snow-free season in summer, other water storage components dominate the gravity residuals. Spring discharge and karst groundwater variations are driven not only by snowmelt and rain but also by glacier melting and permafrost degradation. While the discharge of the Partnach spring and Bockhütte catchments are generally well observed by gauge stations, the estimation of catchment-wide total rainfall amounts and evapotranspiration rates will strongly benefit from including the gravity residuals into the analysis. The high-resolution model of the spatiotemporal variations in the snowpack amount and distribution will be coupled with

a hydrological model to an efficient, physically based, spatially distributed karst snow hydrological model describing relevant physical processes in the RCZ.

Further improvements and enhancements are also planned for the gravimetric part. The set-up of a more detailed and small-scale snowpack description, especially in the direct vicinity of the SG with artificial snow accumulations, is essential in order to increase the sensitivity towards the whole catchment. For this purpose, a high-resolution digital terrain model (DTM) with a grid spacing of  $1 \text{ m} \times 1 \text{ m}$  will be used in the future in combination with a detailed 3D surveying of the buildings at the summit. With regard to atmospheric gravity effects, the complex alpine topography surrounding ZUGOG should be taken into account either by using a weather model with a higher spatial resolution or by setting up a local model based on an array of available barometers (Riccardi et al., 2007). Additional absolute gravity measurements, including amplitude calibrations will improve the SG drift estimation and support long-term studies, while the GNSS station nearby ZUGOG reveals the long-term vertical displacement of the site. It is further intended to install a continuously recording ZLS Burris spring gravimeter in a vertical distance of 500 m below OSG 052 inside Mount Zugspitze in a technical room next to the rails of the cogwheel train to quantify the ongoing mass redistributions and time delays inside the mountain. In addition, the integration of episodic relative gravity measurements both from the tunnel of Mount Zugspitze and from the RCZ, at least 4 times per year with a target uncertainty of  $10 \text{ nm s}^{-2}$  ( $1\sigma$ ), would be highly beneficial in a future hybrid gravimetric approach in order to better capture the spatiotemporal gravity variations on catchment scales and would allow for a more thorough constraining of the hydrological model. A great benefit will be the continuous absolute gravity reference at ZUGOG with known gravity variations and no need to rely on models for the reduction in the relative gravimetric measurements.

The overall research question to be addressed in the future is to what extent the hydro-gravimetric approach contributes to a better understanding and quantification of hydrological processes and storages in this high alpine catchment, with the insights to be transferred to other alpine locations worldwide. Finally, an improved knowledge of hydrological model parameters on catchment scales and possible similar installations in high alpine catchments in the future enhance the resolution of large-scale hydrological variations and reduce the spatial and temporal gap to the satellite mission GRACE-FO (Gravity Recovery and Climate Experiment – Follow On), launched in May 2018, which provides gravity variations with a spatial resolution of  $300 \times 300 \text{ km}^2$  and a temporal resolution of 1 month.

**Data availability.** Raw gravity and atmospheric pressure data from the OSG 052 at ZUGOG have been published (<https://doi.org/10.5880/igets.zu.11.001>, Voigt et al., 2019) and are available from the IGETS database hosted by the Information System and Data Center at GFZ (<https://doi.org/10.2312/gfz.b103-16087>; Voigt et al., 2016a). The subsequent gravity residuals and all auxiliary data from ZUGOG can be provided upon request from the author. The snow water equivalent from the LWD station at the Zugspitzplatz is available from AlpEnDAC (2021; <https://www.alpendac.eu/spa#!/products/badd6e5e-1030-45e8-aefc-a79cc7832a07-01>) after registration.

**Author contributions.** CV conceptualised the paper and took responsibility for the data curation, formal analysis, funding acquisition, investigation, methodology, project administration and visualisation. CV also wrote and prepared the original draft and reviewed and edited the paper with the help of KS, FK and KFW. Moreover, KS, FK and KFW conceptualised the paper and led the investigation. LT, HP, NS and TR curated the data. The project administration was done by TR, HP, NS, CF and FF. LT conducted the formal analysis and reviewed and edited the paper, together with TR, HP, NA, CF and FF. TR, CF and FF were responsible for collecting resources, while CF and FF also took responsibility for the funding acquisition.

**Competing interests.** The authors declare that they have no conflict of interest.

**Disclaimer.** Publisher's note: Copernicus Publications remains neutral with regard to jurisdictional claims in published maps and institutional affiliations.

**Acknowledgements.** The Generic Mapping Tools (GMT; Wessel and Smith, 1998) were used to prepare some figures. The Zugspitze Geodynamic Observatory Germany (ZUGOG) is part of the Modular Earth Science Infrastructure (MESI) of the GFZ. We thank the staff of Umweltforschungsstation Schneefernerhaus, Deutsche

Funkturn, Bayerische Zugspitzbahn and Tiroler Zugspitzbahn, for their personnel and technical support. We also thank Pieter Fourie from the South African Astronomical Observatory (SAAO) for sharing his expertise from Sutherland with us during the installation of the SG at Mount Zugspitze. Bettina Schaeffli, David Crossley and two anonymous reviewers are gratefully acknowledged for their constructive and valuable comments and improvements to the paper.

**Financial support.** The article processing charges for this open-access publication were covered by the Helmholtz Centre Potsdam – GFZ German Research Centre for Geosciences.

**Review statement.** This paper was edited by Bettina Schaeffli and reviewed by two anonymous referees.

## References

- Abe, M., Kroner, C., Förste, C., Petrovic, S., Barthelmes, F., Weise, A., Güntner, A., Creutzfeldt, B., Jahr, T., Wilmes, H., and Wziontek, H.: A comparison of GRACE-derived temporal gravity variations with observations of six European superconducting gravimeters, *Geophys. J. Int.*, 191, 545–556, <https://doi.org/10.1111/j.1365-246X.2012.05641.x>, 2012.
- AlpEnDAC: SSG | Snow Water Equivalent @ Zugspitzplatz LWD Station, [data set], available at: <https://www.alpendac.eu/spa#!/products/badd6e5e-1030-45e8-aefc-a79cc7832a07-01>, last access: 14 September 2021.
- Bahrani, A., Goita, K., and Magagi, R.: Analysing the contribution of snow water equivalent to the terrestrial water storage over Canada, *Hydrol. Process.*, 34, 175–188, <https://doi.org/10.1002/hyp.13625>, 2020.
- Beniston, M., Farinotti, D., Stoffel, M., Andreassen, L. M., Coppola, E., Eckert, N., Fantini, A., Giacona, F., Hauck, C., Huss, M., Huwald, H., Lehning, M., López-Moreno, J.-I., Magnusson, J., Marty, C., Morán-Tejeda, E., Morin, S., Naaim, M., Provenzale, A., Rabatel, A., Six, D., Stötter, J., Strasser, U., Terzago, S., and Vincent, C.: The European mountain cryosphere: a review of its current state, trends, and future challenges, *The Cryosphere*, 12, 759–794, <https://doi.org/10.5194/tc-12-759-2018>, 2018.
- Bernhardt, M., Härer, S., Feigl, M., and Schulz, K.: Der Wert Alpiner Forschungseinzugsgebiete im Bereich der Fernerkundung, der Schneedeckenmodellierung und der lokalen Klimamodellierung, *Österr. Wasser- und Abfallw.*, 70, 515–528, <https://doi.org/10.1007/s00506-018-0510-8>, 2018.
- Boy, J.-P.: EOST Loading Service, [data set], <http://loading.u-strasbg.fr> (last access: 30 April 2021), 2021.
- Boy, J.-P., Barriot, J.-P., Förste, C., Voigt, C., and Wziontek, H.: Achievements of the first 4 years of the International Geodynamics and Earth Tide Service (IGETS) 2015–2019, IAG Symp., [https://doi.org/10.1007/1345\\_2020\\_94](https://doi.org/10.1007/1345_2020_94), 2020.
- Carbone, D., Cannavò, F., Greco, F., Reineman, R., and Warburton, R. J.: The Benefits of Using a Network of Superconducting Gravimeters to Monitor and Study Active Volcanoes, *J. Geophys. Res.-Sol. Ea.*, 123, 2153–2165, <https://doi.org/10.1029/2018JB017204>, 2019.

- Chaffaut, Q., Hinderer, J., Masson, F., Viville, D., Pasquet, S., Boy, J. P., Bernard, J. D., Lesparre, N., and Pierret, M. C.: New insights on water storage dynamics in a mountainous catchment from superconducting gravimetry, *Geophys. J. Int.*, <https://doi.org/10.1093/gji/ggab328>, accepted, 2021.
- Creutzfeldt, B., Güntner, A., Klügel, T., and Wziontek, H.: Simulating the influence of water storage changes on the superconducting gravimeter of the Geodetic Observatory Wettzell, Germany, *Geophysics*, 73, WA95–WA104, <https://doi.org/10.1190/1.2992508>, 2008.
- Creutzfeldt, B., Troch, P., Güntner, A., Ferré, T. P. A., Graeff, T., and Merz, B.: Storage-discharge relationships at different catchment scales based on local high-precision gravimetry, *Hydrol. Process.*, 28, 1465–1475, <https://doi.org/10.1002/hyp.9689>, 2013.
- Crossley, D.: GGP Decimation Filters, <http://www.eas.slu.edu/GGP/ggpfilters.html> (last access: 11 November 2020), created 27 March 2007, updated 19 April 2010, 2020.
- Delobbe, L., Watlet, A., Wilfert, S., and Van Camp, M.: Exploring the use of underground gravity monitoring to evaluate radar estimates of heavy rainfall, *Hydrol. Earth Syst. Sci.*, 23, 93–105, <https://doi.org/10.5194/hess-23-93-2019>, 2019.
- Dobslaw, H., Bergmann-Wolf, I., Dill, R., Poropat, L., Thomas, M., Dahle, C., Esselborn, S., König, R., and Flechtner, F.: A new high-resolution model of non-tidal atmosphere and ocean mass variability for de-aliasing of satellite gravity observations: AOD1B RL0., *Geophys. J. Int.*, 211, 263–269, <https://doi.org/10.1093/gji/ggx302>, 2017.
- Fores, B., Champollion, C., Le Moigne, N., Bayer, R., and Chéry, J.: Assessing the precision of the iGrav superconducting gravimeter for hydrological models and karstic hydrological process identification. *Geophys. J. Int.*, 208, 269–280, <https://doi.org/10.1093/gji/ggw396>, 2017.
- Förste, C., Voigt, C., Abe, M., Kroner, C., Neumeyer, J., Pflug, H., and Fourie, P.: Superconducting Gravimeter Data from Sutherland – Level 1, GFZ Data Services [data set], <https://doi.org/10.5880/igets.su.11.001>, 2016.
- Galleman, T., Haas, U., Teipel, U., von Poschinger, A., Wagner, B., Mahr, M., and Bäse, F.: Permafrost-Messstation am Zugspitzgipfel: Ergebnisse und Modellberechnungen, *Umwelt-Spezial, Geologica Bavaria 115*, Bayerisches Landesamt für Umwelt (LfU), Augsburg, Germany, 2017.
- Galleman, T., Wagner, B., Foltyn, M., Mahr, M., and Jerz, H.: Permafrost und Böden im Bereich der Zugspitze, *UmweltSpezial, Geologica Bavaria 120*, Bayerisches Landesamt für Umwelt (LfU), Augsburg, Germany, 2021.
- Gelaro, R., McCarty, W., Suárez, M. J., Todling, R., Molod, A., Takacs, L., Randles, C. A., Darmenov, A., Bosilovich, M. G., Reichle, R., Wargan, K., Coy, L., Cullather, R., Draper, C., Akella, S., Buchard, V., Conaty, A., da Silva, A. M., Gu, W., Kim, G.-K., Koster, R., Lucchesi, R., Merkova, D., Nielsen, J. E., Parityka, G., Pawson, S., Putman, W., Rienecker, M., Schubert, S. D., Sienkiewicz, M., and Zhao, B.: The Modern-Era Retrospective Analysis for Research and Applications, Version 2 (MERRA-2), *J. Climate*, 30, 5419–5454, <https://doi.org/10.1175/JCLI-D-16-0758.1>, 2017.
- Grünwald, T., Stötter, J., Pomeroy, J. W., Dadic, R., Moreno Baños, I., Marturià, J., Spross, M., Hopkinson, C., Burlando, P., and Lehning, M.: Statistical modelling of the snow depth distribution in open alpine terrain, *Hydrol. Earth Syst. Sci.*, 17, 3005–3021, <https://doi.org/10.5194/hess-17-3005-2013>, 2013.
- Güntner, A., Reich, M., Mikolaj, M., Creutzfeldt, B., Schroeder, S., and Wziontek, H.: Landscape-scale water balance monitoring with an iGrav superconducting gravimeter in a field enclosure, *Hydrol. Earth Syst. Sci.*, 21, 3167–3182, <https://doi.org/10.5194/hess-21-3167-2017>, 2017.
- Gurtz, J., Baltensweiler, A., and Lang, H.: Spatially distributed hydrotope-based modelling of evapotranspiration and runoff in mountainous basins, *Hydrol. Process.*, 13, 2751–2768, [https://doi.org/10.1002/\(SICI\)1099-1085\(19991215\)13:17,%3C2751::AID-HYP897%3E3.0.CO;2-O](https://doi.org/10.1002/(SICI)1099-1085(19991215)13:17,%3C2751::AID-HYP897%3E3.0.CO;2-O), 1999.
- Hagg, W., Mayer, C., Mayr, E., and Heilig, A.: Climate and glacier fluctuations in the Bavarian Alps in the past 120 years, *Erdkunde*, 66, 121–142, 2012.
- Härer, S., Bernhardt, M., Corripio, J. G., and Schulz, K.: PRAC-TISE – Photo Rectification And ClassificaTion SoftwarE (V.1.0), *Geosci. Model Dev.*, 6, 837–848, <https://doi.org/10.5194/gmd-6-837-2013>, 2013.
- Härer, S., Bernhardt, M., and Schulz, K.: PRACTISE – Photo Rectification And ClassificaTion SoftwarE (V.2.1), *Geosci. Model Dev.*, 9, 307–321, <https://doi.org/10.5194/gmd-9-307-2016>, 2016.
- Härer, S., Bernhardt, M., Siebers, M., and Schulz, K.: On the need for a time- and location-dependent estimation of the NDSI threshold value for reducing existing uncertainties in snow cover maps at different scales, *The Cryosphere*, 12, 1629–1642, <https://doi.org/10.5194/tc-12-1629-2018>, 2018.
- Hinderer, J., Crossley, D., and Warburton, R.: Superconducting Gravimetry, in: *Treatise on Geophysics*, 2nd edition, edited by: Gerald Schubert, Elsevier, Oxford, 3, 59–115, <https://doi.org/10.1016/B978-0-444-53802-4.00062-2>, 2015.
- Hürkamp, K., Zentner, N., Reckerth, A., Weishaupt, S., Wetzel, K.-F., Tschiersch, J., and Stumpp, C.: Spatial and temporal variability of snow isotopic composition on Mt. Zugspitze, Bavarian Alps, Germany, *J. Hydrol. Hydromech.*, 67, 49–58, <https://doi.org/10.2478/johh-2018-0019>, 2019.
- Immerzeel, W. W., Lutz, A. F., Andrade, M., Bahl, A., Biemans, H., Bolch, T., Hyde, S., Brumby, S., Davies, B. J., Elmore, A. C., Emmer, A., Feng, M., Fernández, A., Haritashya, U., Kargel, J. S., Koppes, M., Kraaijenbrink, P. D. A., Kulkarni, A. V., Mayewski, P. A., Nepal, S., Pacheco, P., Painter, T. H., Pellicciotti, F., Rajaram, H., Rupper, S., Sinisalo, A., Shrestha, A. B., Viviroli, D., Wada, Y., Xiao, C., Yao, T., and Baillie, J. E. M.: Importance and vulnerability of the world’s water towers, *Nature*, 577, 364–369, <https://doi.org/10.1038/s41586-019-1822-y>, 2020.
- IPCC: Climate Change 2014: Synthesis Report, Contribution of Working Groups I, II and III to the Fifth Assessment Report of the Intergovernmental Panel on Climate Change, edited by: Core Writing Team, Pachauri, R. K., and Meyer, L. A., IPCC, Geneva, Switzerland, 151 pp., 2014.
- Kennedy, J., Ferré, T. P. A., Güntner, A., Abe, M., and Creutzfeldt, B.: Direct measurement of subsurface mass change using the variable baseline gravity gradient method, *Geophys. Res. Lett.*, 41, 2827–2834, <https://doi.org/10.1002/2014GL059673>, 2014.
- Klügel, T. and Wziontek, H.: Correcting gravimeters and tiltmeters for atmospheric mass attraction using op-

- erational weather models, *J. Geodyn.*, 48, 204–210, <https://doi.org/10.1016/j.jog.2009.09.010>, 2009.
- Krautblatter, M., Verleysdonk, S., Flores-Orozco, A., and Kemna, A.: Temperature-calibrated imaging of seasonal changes in permafrost rock walls by quantitative electrical resistivity tomography (Zugspitze, German/Austrian Alps), *J. Geophys. Res.*, 115, F02003, <https://doi.org/10.1029/2008JF001209>, 2010.
- Lamb, R. and Beven, K.: Using interactive recession curve analysis to specify a general catchment storage model, *Hydrol. Earth Syst. Sci.*, 1, 101–113, <https://doi.org/10.5194/hess-1-101-1997>, 1997.
- Lauber, U. and Goldscheider, N.: Use of artificial and natural tracers to assess groundwater transit-time distribution and flow systems in a high-alpine karst system (Wetterstein Mountains, Germany), *Hydrogeol. J.*, 22, 1807–1824, <https://doi.org/10.1007/s10040-014-1173-6>, 2014.
- Lehning, M., Völksch, I., Gustafsson, D., Nguyen, T., Stähli, M., and Zappa, M.: ALPINE3D: A detailed model of mountain surface processes and its application to snow hydrology, *Hydrol. Process.*, 20, 2111–2128, <https://doi.org/10.1002/hyp.6204>, 2006.
- Marsh, C. B., Pomeroy, J. W., and Wheeler, H. S.: The Canadian Hydrological Model (CHM) v1.0: a multi-scale, multi-extent, variable-complexity hydrological model – design and overview, *Geosci. Model Dev.*, 13, 225–247, <https://doi.org/10.5194/gmd-13-225-2020>, 2020.
- Mayer, C., Hagg, W., Weber, M., and Lambrecht, A.: Zukunft ohne Eis, Zweiter Bayerischer Gletscherbericht: Klimawandel in den Alpen, Bayerische Akademie der Wissenschaften (BAdW), München, Germany, 2021.
- Mikolaj, M., Meurers, B., and Güntner, A.: Modelling of global mass effects in hydrology, atmosphere and oceans on surface gravity, *Comput. Geosci.*, 93, 12–20, <https://doi.org/10.1016/j.cageo.2016.04.014>, 2016.
- Mikolaj, M., Reich, M., and Güntner, A.: Resolving Geophysical Signals by Terrestrial Gravimetry: A Time Domain Assessment of the Correction-Induced Uncertainty, *J. Geophys. Res.-Sol. Ea.*, 124, 2153–2165, <https://doi.org/10.1029/2018JB016682>, 2019.
- Morche, D. and Schmidt, K.-H.: Sediment transport in an alpine river before and after a dambreak flood event, *Earth Surf. Proc. Land.*, 37, 347–353, <https://doi.org/10.1002/esp.2263>, 2012.
- Naujoks, M., Kroner, C., Weise, A., Jahr, T., Krause, P., and Eisner, S.: Evaluating local hydrological modelling by temporal gravity observations and a gravimetric three-dimensional model, *Geophys. J. Int.*, 182, 233–249, <https://doi.org/10.1111/j.1365-246X.2010.04615.x>, 2010.
- Peters, T., Schmeer, M., Flury, J., and Ackermann, C.: Erfahrungen im Gravimeterkalibriersystem Zugspitze, *zfv, Augsburg, Germany*, 3/2019, 2009.
- Pomeroy, J., Bernhardt, M., and Marks, D.: Research network to track alpine water, *Nature*, 521, p. 32, <https://doi.org/10.1038/521032c>, 2015.
- Ramatschi, M., Bradke, M., Nischan, T., and Männel, B.: GNSS data of the global GFZ tracking network, GFZ Data Services [data set], <https://doi.org/10.5880/GFZ.1.1.2020.001>, 2019.
- Rappl, A., Wetzol, K.-F., Büttner, G., and Scholz, M.: Tracerhydrologische Untersuchungen am Partnach-Ursprung, *Hydrol. Wasserbewirts.*, 54, 222–230, 2010.
- Scandroglio, R., Heinze, M., Schröder, T., Pail, R., and Krautblatter, M.: A first attempt to reveal hydrostatic pressure in permafrost-affected rock slopes with relative gravimetry, *Geophysical Research Abstracts*, 21, EGU2019-12870, 2019.
- Riccardi, U., Hinderer, J., and Boy, J.-P.: On the efficiency of barometric arrays to improve the reduction of atmospheric effects on gravity data, *Phys. Earth Planet. In.*, 161, 224–242, <https://doi.org/10.1016/j.pepi.2007.02.007>, 2007.
- Schäfer, F., Jousset, P., Güntner, A., Erbas, K., Hinderer, J., Rosat, S., Voigt, C., Schöne, T., and Warburton, R.: Performance of three iGrav superconducting gravity meters before and after transport to remote monitoring sites, *Geophys. J. Int.*, 223, 959–972, <https://doi.org/10.1093/gji/ggaa359>, 2020.
- Timmen, L., Flury, J., Peters, T., and Gitlein, O.: 2006. A new absolute gravity base in the German Alps, in: *Contributions to Geophysics and Geodesy*, 36, no.SI WIGFR, 7–20, 2006.
- Timmen, L., Rothleitner, C., Reich, M., Schröder, S., and Cieslak, M.: Investigation of Scintrex CG-6 Gravimeters in the Gravity Meter Calibration System Hannover, *AVN*, 127, 155–162, 2020.
- Timmen, L., Gerlach, C., Rehm, T., Völkse, C., and Voigt, C.: Geodetic-gravimetric monitoring for mountain uplift and hydrological variations at Zugspitze and Wank, *Remote Sens.*, 13, 918, <https://doi.org/10.3390/rs13050918>, 2021.
- Van Camp, M. and Vauterin, P.: Tsoft: graphical and interactive software for the analysis of time series and Earth tides, *Comput. Geosci.*, 31, 631–640, <https://doi.org/10.1016/j.cageo.2004.11.015>, 2005.
- Van Camp, M., de Viron, O., Pajot-Métivier, G., Casenave, F., Watlet, A., Dassargues, A., and Vanclooster, M.: Direct measurement of evapotranspiration from a forest using a superconducting gravimeter, *Geophys. Res. Lett.*, 43, 10225–10231, <https://doi.org/10.1002/2016GL070534>, 2016.
- Viviroli, D., Dürr, H. H., Messerli, B., Meybeck, M., and Weingartner, R.: Mountains of the world, water towers for humanity: Typology, mapping, and global significance, *Water Resour. Res.*, 43, W07447, <https://doi.org/10.1029/2006WR005653>, 2007.
- Voigt, C., Förste, C., Wziontek, H., Crossley, D., Meurers, B., Palinkas, V., Hinderer, J., Boy, J.-P., Barriot, J.-P., and Sun, H.: Report on the data base of the international geodynamics and earth tide service (IGETS), Scientific technical report STR Potsdam, GFZ German Research Centre for Geosciences [data set], Potsdam, Germany, <https://doi.org/10.2312/gfz.b103-16087>, 2016a.
- Voigt, C., Denker, H., and Timmen, L.: Time-variable gravity potential components for optical clock comparisons and the definition of international time scales, *Metrologia*, 53, 1365–1383, <https://doi.org/10.1088/0026-1394/53/6/1365>, 2016b.
- Voigt, C., Pflug, H., Förste, C., Flechtner, F., and Rehm, T.: Superconducting Gravimeter Data from Zugspitze – Level 1, GFZ Data Services, <https://doi.org/10.5880/igets.zu.11.001>, 2019.
- Watlet A., Van Camp M., Francis O., Poulain A., Rochez G., Hallet V., Quinif Y., and Kaufmann O.: Gravity monitoring of underground flash flood events to study their impact on groundwater recharge and the distribution of karst voids, *Water Resour. Res.*, 56, e2019WR026673, <https://doi.org/10.1029/2019WR026673>, 2020.
- Weber, M., Bernhardt, M., Pomeroy, J. W., Fang, X., Härer, S., and Schulz, K.: Description of current and future snow processes in a

- small basin in the Bavarian Alps, *Environ. Earth Sci.*, 75, 1223, <https://doi.org/10.1007/s12665-016-6027-1>, 2016.
- Weber, M., Feigl, M., Schulz, K., and Bernhardt, M.: On the Ability of LIDAR Snow Depth Measurements to Determine or Evaluate the HRU Discretization in a Land Surface Model, *Hydrology*, 7, 20, <https://doi.org/10.3390/hydrology7020020>, 2020.
- Weber, M., Koch, F., Bernhardt, M., and Schulz, K.: The evaluation of the potential of global data products for snow hydrological modelling in ungauged high-alpine catchments, *Hydrol. Earth Syst. Sci.*, 25, 2869–2894, <https://doi.org/10.5194/hess-25-2869-2021>, 2021.
- Wenzel, H.-G.: ETERNA Version 3.40, Earth Tide Data Processing Package ETERNA, Black Forest Observatory, Universität Karlsruhe [code], 1997.
- Wessel, P. and Smith, F.: New, improved version of generic mapping tools released, *EOS*, 79, 579, <https://doi.org/10.1029/98EO00426>, 1998.
- Wetzel, K.-F.: On the hydrology of the Partnach area in the Wetterstein mountains (Bavarian Alps), *Erdkunde*, 58, 172–186, 2004.
- Wilmes, H., Wziontek, H., Falk, R., and Bonvalot, S.: AGrav – The New International Absolute Gravity Database of BGI and BKG and its benefit for the Global Geodynamics Project (GGP), *J. Geodyn.*, 48, 305–309, <https://doi.org/10.1016/j.jog.2009.09.035>, 2009.